$\gamma\gamma \to t\bar{c} + c\bar{t}$ in a supersymmetric theory with an explicit R-parity violation *

Yu Zeng-Hui [a,c] Herbert Pietschmann [a] Ma Wen-Gan [b,c] Han Liang [c] Jiang Yi [c]

[a]Institut für Theoretische Physik, Universität Wien, A-1090 Vienna, Austria

[b]CCAST (World Laboratory), P.O.Box 8730, Beijing 100080,P.R.China

[c]Department of Modern Physics, University of Science and Technology of China (USTC), Hefei, Anhui 230027, P.R.China

ABSTRACT

We studied the process $\gamma\gamma \to t\bar{c}+c\bar{t}$ in a R_p violating supersymmetric Model with the effects from both B- and L-violating interactions. The calculation shows that it is possible to detect a R_p violating signal at the Linear Collider. Information about the B-violating interaction in this model could be obtained under very clean background, if we take the present upper bounds for the parameters in the supersymmetric $\not{R}_p$ interactions. Even if we can not detect a signal of $\not{R}_p$ in the experiment, we may get more stringent constraints on the heavy-flavor $\not{R}_p$ couplings.

PACS number(s): 13.65.+i, 13.88.+e, 14.65.-q, 14.80.Dq, 14.80.Gt

*Supported in part by Committee of National Natural Science Foundation of China and Project IV.B.12 of scientific and technological cooperation agreement between China and Austria

I. Introduction

The minimal supersymmetric model (MSSM)[1] is one of the most interesting extensions of the Standard Model (SM) and is considered as the most favorable model beyond SM. Thus, it is interesting to confirm whether R-parity(R_p), which is introduced to guarantee the B- and L-conservation automatically, is conserved in the supersymmetric extension of the SM [2]. Because of the lack of credible theoretical arguments and experimental tests for R_p conservation, we can say that the R_p violation ($\not{R}_p$)would be equally well motivated in the supersymmetric extension of the SM [3]. Since in the R_p-violation models supersymmetry particles can be singly producted and neutrinos would get masses and mixing [4], it is a significant source of new physics. Especially after the first signals for neutrino oscillations from atmospheric neutrinos were observed in Super-Kamiokande [5] and an anomaly was detected in HERA e^+p deep inelastic scattering(DIS) [6], R_p-violation can be a good candidate to explain those experimental results.

In the last few years, many efforts were made to find $\not{R}_p$ interactions in experiments. Unfortunately, up to now we have only some upper limits on $\not{R}_p$ parameters, such as B-violating $\not{R}_p$ parameters ($\lambda^{''}$) and L-violating $\not{R}_p$ parameters(λ and $\lambda^{'}$)[4][7] and results are colletec in Ref. [8] (The parameters will be defined clearly in the following sector). Therefore, trying to find the signal of R_p violation or getting more stringent constraints on the parameters in future experiments, is a promising task. Possible ways to find a R_p violation signal can be detecting odd number supersymmetric particle interactions as a direct signal or testing discrepancies between predictions of R_p-conservation models and

R_p-violation models in the experiments as indirect informations.

In our paper we will consider the process $e^+e^- \to \gamma\gamma \to t\bar{c} + c\bar{t}$ in the future Linear Collider(LC). This rare process, which is supressed by the GIM mechanism in the Standard Model [9], can be a good window to open new physics. In Ref. [10], it was pointed out that anomalous $t\bar{q}\gamma$ coupling admitted by present experimental results can be much larger than the prediction of SM. Thus, R_p-violation can be a significant source which gives this anomalous coupling. Although small values of $\lambda^{'}$ and $\lambda^{''}$ in $\not{R}_p$ theory would suppress this process, the present upper bounds on $\not{R}_p$ parameters still admit experimental observation ($\lambda^{'}$ and $\lambda^{"}$ can be of order 1 when they involve heavy flavors, which is reasonable with assumption of family symmetry [11]). So we can hope that this process allows detection of R_p violation within the present parameter upper limits.

With the advent of new collider techniques, we can produce highly coherent laser beams being back-scattered with high luminosity and efficiency at the e^+e^- colliders[12]. The $\gamma\gamma$ collisions give us a very clean environment to study the $t\bar{c}$(or $c\bar{t}$) production. Effects of L-violating parameters in the e^+e^- collisions have been studied[7], but only little attention was paid to B-violating parameters[13]. The process considered here, can give us a chance to detect $B - violating$ parameters $\lambda^{''}$ in a very *clean* environment. We can also get information on the parameter $\lambda^{'}$ from the process, especially for heavy flavors, which are only weakly constrained by present data.

Even without R_p violation, there are flavor-changing mechanisms[14] in the MSSM, e.g.squark mixing. Therefore, R_p violation in $\gamma\gamma \to t\bar{c} + c\bar{t}$ can only be established if it

exceeds the value of these other mechanisms. Fortunately, in most models with universal SUSY breaking, those contributions are small(for details see ref. [14]). Hence we shall assume that they are suppressed throughout our paper.

Other possible competing mechanism, such as Two-Higgs-Doublet-Model(THDM), was considered by Atwood et al. [15] and Y.Jiang et al. [15]. The results showed that the cross section would be much smaller assuming the masses of higgses to be far from the c.m. energy of colliders, so we can distinguish them easily from R_p-violation interactions.

In this work we concentrate on the process $e^+e^- \to \gamma\gamma \to t\bar{c} + c\bar{t}$ in the R-parity violating supersymmetric theory. In section 2, we give the supersymmetric $\not{R}_p$ interactions. In section 3 we give the analytical calculations of $\gamma\gamma \to t\bar{c} + c\bar{t}$. In section 4 the numerical results of the process $e^+e^- \to \gamma\gamma \to t\bar{c} + c\bar{t}$ are presented. The conclusion is given in section 5 and some details of the expressions are listed in the appendix.

II. R-parity violation($\not{R}_p$) in MSSM

All renormalizable supersymmetric $\not{R}_p$ interactions can be introduced in the superpotential[8]:

$$W_{\not{R}_p} = \frac{1}{2}\lambda_{[ij]k} L_i . L_j \bar{E}_k + \lambda'_{ijk} L_i . Q_j \bar{D}_k + \frac{1}{2}\lambda''_{i[jk]} \bar{U}_i \bar{D}_j \bar{D}_k + \epsilon_i L_i H_u . \tag{2.1}$$

where L_i, Q_i and H_u are SU(2) doublets containing lepton, quark and Higgs superfields respectively, $\bar{E}_j$ ($\bar{D}_j$, $\bar{U}_j$) are the singlets of lepton (down-quark and up-quark), and i, j, k are generation indices and square brackets on them denote antisymmetry in the bracketted indices.

We ignored the last term in Eq(2.1), which will introduce mixing of leptons and Higgses, since its effects are rather small in our process [4][**?**]. So we have 9 λ-type, 27 $\lambda^{'}$-type and 9 $\lambda^{''}$-type independent parameters left. The Lagrangian density of $\not{R}_p$ is given as follows: (the lowest order of λ)

$$L_{\not{R}_p} = L^{\lambda}_{\not{R}_p} + L^{\lambda^{'}}_{\not{R}_p} + L^{\lambda^{''}}_{\not{R}_p} \tag{2.2}$$

$$L^{\lambda}_{\not{R}_p} = \lambda_{[ij]k}[\tilde{\nu}_{iL}\bar{e}_{kR}e_{jL} + \tilde{e}_{jL}\bar{e}_{kR}\nu_{iL} + \tilde{e}^{*}_{kR}\overline{\nu^{c}_{iL}}e_{jL} - \tilde{\nu}_{jL}\bar{e}_{kR}e_{iL} - \tilde{e}_{iL}\bar{e}_{kR}\nu_{jL} - \tilde{e}^{*}_{kR}\overline{\nu^{c}_{jL}}e_{iL}] + h.c.$$

$$L^{\lambda^{'}}_{\not{R}_p} = \lambda^{'}_{ijk}[\tilde{\nu}_{iL}\bar{d}_{kR}d_{jL} + \tilde{d}_{jL}\bar{d}_{kR}\nu_{iL} + \tilde{d}^{*}_{kR}\overline{\nu^{c}_{iL}}d_{jL} - \tilde{e}_{iL}\bar{d}_{kR}u_{jL} - \tilde{u}_{jL}\bar{d}_{kR}e_{jL} - \tilde{d}^{*}_{kR}\overline{e^{c}_{iL}}u_{jL}] + h.c.$$

$$L^{\lambda^{"}}_{\not{R}_p} = \lambda^{"}_{i[jk]}\epsilon_{\alpha\beta\gamma}[\tilde{u}^{*}_{iR\alpha}\bar{d}_{kR\beta}d^{c}_{jR\gamma} + \tilde{d}^{*}_{jR\beta}\bar{u}_{iR\alpha}d^{c}_{kR\gamma} + \tilde{d}^{*}_{kR\gamma}\bar{u}_{iR\alpha}d^{c}_{jR\beta}] + h.c. \tag{2.3}$$

The proton lifetime suppresses the possibility of both B-violation and L-violation, leading to the constraints:[8]

$$|(\lambda \; or \; \lambda^{'})\lambda^{"}| < 10^{-10}(\frac{\tilde{m}}{100GeV})^{2}. \tag{2.4}$$

where $\tilde{m}$ is the mass of super quark or super lepton. Therefore, we consider the contributions from $L^{\lambda^{'}}_{\not{R}_p}$ and $L^{\lambda^{"}}_{\not{R}_p}$ separately. Although the individual parameters λ, $\lambda^{'}$ and $\lambda^{"}$ should be typically less than $10^{-1} - 10^{-2}(\frac{\tilde{m}}{100GeV})^{2}$[8], we can expect the parameters

involving heavy flavors to be much larger in analogy with the Yukawa couplings in the MSSM[11]. Since the constraints on such parameters from present experimental data are rather weak, testing $\not{R}_p$ at high energy is still very important.

III. Calculations

In the following calculations we assume the parameters $\lambda^{'}$ and $\lambda^{''}$ to be real. One-loop corrections (as shown in Fig.1) of $\gamma(p_3)\gamma(p_4) \to t(p1)\bar{c}(p2)$ can be split into the following components:

$$M = \delta M_s + \delta M_v + \delta M_b. \tag{3.1}$$

where δM_s, δM_v and δM_b are the one-loop amplitudes corresponding to the self-energy, vertex, and box correction diagrams respectively. We find that amplitudes are proportional to the products $\lambda^{'}_{i2j}\lambda^{'}_{i3j}$ $(i,j = 1,2,3)$ (Fig.1.(a.1-2),Fig.1.(b.1-4) and Fig.1.(c.1-8)) and $\lambda^{"}_{2ij}\lambda^{"}_{3ij}(i,j = 1,2,3)$ (Fig.1.(a.3),Fig.1.(b.5-6) and Fig.1.(c.9-12)); thus it is possible to detect $\not{R}_p$ signals or get much stronger constraints on those parameters by measuring this process in future LC experiments.

We define the Mandelstam variables as usual

$$\hat{s} = (p_1 + p_2)^2 = (p_3 + p_4)^2 \tag{3.2}$$

$$\hat{t} = (p_1 - p_3)^2 = (p_4 - p_2)^2 \tag{3.2}$$

$$\hat{u} = (p_1 - p_4)^2 = (p_3 - p_2)^2 \tag{3.4}$$

The $t\bar{c} + c\bar{t}$ productions via $\gamma\gamma$ fusion obtains contributions only from one-loop Feynman diagrams at the lowest order. Since the proper vertex counterterm should cancel with

the counterterms of the external legs diagrams in this case, we do not need to deal with the ultraviolet divergence. Thus we simply sum over all (unrenormalized) reducible and irreducible diagrams and the result is finite and gauge invariant. In the Appendix we will give the details of the amplitudes. Similarly, we can get the amplitude for subprocess $\gamma\gamma \to c\bar{t}$. Collecting all terms in Eq.(3.1), we obtain the total cross section for the subprocess $\gamma\gamma \to t\bar{c} + c\bar{t}$:

$$\hat{\sigma}(\hat{s}) = \frac{2N_c}{16\pi\hat{s}^2}\int_{\hat{t}^-}^{\hat{t}^+} d\hat{t}\bar{\sum}_{spins}[|M|^2], \tag{3.5}$$

where $\hat{t}^{\pm} = \frac{1}{2}\left[(m_t^2 + m_c^2 - \hat{s}) \pm \sqrt{\hat{s}^2 + m_t^4 + m_c^4 - 2\hat{s} * m_t^2 - 2\hat{s} * m_c^2 - 2m_t^2 * m_c^2}\right]$, colour factor $N_c = 3$ and the bar over summation means averaging over initial spins. In order to get the observable results in the measurements of $t\bar{c} + \bar{t}c$ production via $\gamma\gamma$ fusion in e^+e^- collider, we need to fold the cross section of $\gamma\gamma \to t\bar{c} + c\bar{t}$ with the photon luminosity,

$$\sigma(s) = \int_{(m_t+m_c)/\sqrt{s}}^{x_{max}} dz \frac{dL_{\gamma\gamma}}{dz}\hat{\sigma}(\hat{s}), \tag{3.6}$$

where $\hat{s} = z^2 s$, $\sqrt{s}$ and $\sqrt{\hat{s}}$ are the e^+e^- and $\gamma\gamma$ CMS energies respectively, and $\frac{dL_{\gamma\gamma}}{dz}$ is the photon luminosity, which is defined as[12]

$$\frac{dL_{\gamma\gamma}}{dz} = 2z\int_{z^2/x_{max}}^{x_{max}} \frac{dx}{x} F_{\gamma/e}(x)F_{\gamma/e}(z^2/x). \tag{3.7}$$

The energy spectrum of the back-scattered photon is given by [12].

$$F_{\gamma/e}(x) = \frac{1}{D(\xi)}[1 - x + \frac{1}{1-x} - \frac{4x}{\xi(1-x)} + \frac{4x^2}{\xi^2(1-x)^2}]. \tag{3.8}$$

taking the parameters of Ref.[17], we have $\xi = 4.8$, $x_{max} = 0.83$ and $D(\xi) = 1.8$.

IV. Numerical results

In the numerical calculations, we assume $m_{\tilde{q}} = m_{\tilde{l}}$ and consider the effects from $L^{\lambda^{'}}_{\not R_p}$ and $L^{\lambda^{"}}_{\not R_p}$ separately. It will be no loss of generality and the results could be kept in realistic models of supersymmetry.

For the B-violating parameter $\lambda^{"}_{2ij}\lambda^{"}_{3ij}(i,j=1-3)$, upper bounds of $\lambda^{"}_{223}$ and $\lambda^{"}_{323}$ dominate all others, so we will neglect all other $\lambda^{"}$ terms. For the L-violating parameter $\lambda^{'}_{i2j}\lambda^{'}_{i3j}(i,j=1-3)$, we neglect all parameters except for $\lambda^{'}_{323}$ and $\lambda^{'}_{333}$.

In Fig.2, we show the cross section of $e^+e^- \to \gamma\gamma \to t\bar{c} + c\bar{t}$ as function of c.m. energy of the electron-positron system at the upper bounds of $\lambda^{"}$, i.e. $\lambda^{"}_{323}\lambda^{"}_{223} = 0.625$, see Ref.[4]. We take $m_{\tilde{l}} = m_{\tilde{q}} = 100\ GeV$ (Solid line) and $m_{\tilde{l}} = m_{\tilde{q}} = 150\ GeV$ (Dashed line), respectively. The results show that the cross section can be 0.64 fb for solid line(0.29 fb for dashed line) when the c.m. energy ($\sqrt{s}$) is equal to 500 GeV. So if the electron-positron integrated luminosity of the LC is $50fb^{-1}$, we can get about 32 events per year when $m_{\tilde{l}} = m_{\tilde{q}} = 100\ GeV$. Therefore the $\not R_p$ signal could be detected, if $\lambda^{''}$ are large enough under the present allowed upper bounds.

In Fig.3, we plot the cross section of $e^+e^- \to \gamma\gamma \to t\bar{c} + c\bar{t}$ as function of c.m. energy of the electron-positron system with the upper bounds of $\lambda^{'}$, i.e. $\lambda^{'}_{333}\lambda^{'}_{323} = 0.096$, see Ref.[4]. We take again $m_{\tilde{l}} = m_{\tilde{q}} = 100\ GeV$ for solid line and $m_{\tilde{l}} = m_{\tilde{q}} = 150\ GeV$ for dashed line, respectively. The cross section is much smaller than that of Fig.2. That looks reasonable because the upper limits of $\lambda^{'}$ from present data are much smaller than those of $\lambda^{''}$. The cross section can be only about 0.017 fb when $\sqrt{s} = 500GeV$, that means we

can get only 1 event per year at the LC with integrated luminosity 50 fb^{-1}. Thus it will be difficult to find the signal of $\lambda^{'}$ from the process which we discussed.

In order to give more stringent constraints of $\lambda^{''}$ in future experiments, we draw the cross section at $\sqrt{s} = 500\ GeV$ as function of $\lambda^{''}_{223}\lambda^{''}_{323}$ in Fig.4(Solid line is for $m_{\tilde{l}} = m_{\tilde{q}} = 100\ GeV$ and dashed-line for $m_{\tilde{l}} = m_{\tilde{q}} = 150\ GeV$). When $\lambda^{''}_{223}\lambda^{''}_{323}$ is about 0.1, the cross section will be about 0.02 fb. That corresponds to 1 event per year at the LC. So if we can't get the signal of $\not{R}_p$ from the experiments, we can set the stronger constraint on $\lambda^{''}_{223}$ and $\lambda^{''}_{323}$, i.e. $\lambda^{''}_{223}\lambda^{''}_{323} \leq 0.1$.

Similarly we draw the relation between the cross section and the parameter product $\lambda^{'}_{323}\lambda^{'}_{333}$ with $\sqrt{s} = 500\ GeV$ in Fig.5, solid line is for $m_{\tilde{l}} = m_{\tilde{q}} = 100\ GeV$ and dashed-line for $m_{\tilde{l}} = m_{\tilde{q}} = 150\ GeV$.

IV. Conclusion

We studied both the subprocess $\gamma\gamma \rightarrow t\bar{c} + c\bar{t}$ and process $e^+e^- \rightarrow \gamma\gamma \rightarrow t\bar{c} + c\bar{t}$ in one-loop order in explicit $\not{R}_p$ supersymmetric model. The calculations show that we can test $\not{R}_p$ theory in the future LC experiments, if the B-violating couplings($\lambda^{''}$-type) are large enough within the present experimentally admitted range. That means we can detect B-violating interactions in the lepton colliders with cleaner background. We also consider the effect from L-violating interactions ($\lambda^{'}$-type), and conclude that it is very small in this process.

From our calculation, we find that the subprocess $\gamma\gamma \rightarrow t\bar{c} + c\bar{t}$ is very helpful in

getting the information about the B-violating couplings($\lambda^{''}$). That is because the effect of L-violating interactions($\lambda^{'}$) is small and can be neglected. Thus if we can observe events of this process in the LC, we can conclude that they are from B-violation couplings. Even if we can't detect any signal from the experiments, we could improve the present upper bounds on $\lambda^{''}_{223}\lambda^{''}_{323}$.

The authors would like to thank Prof.H.Stremnitzer for reading the manuscript.

Appendix

A. Loop integrals:

We adopt the definitions of two-, three-, four-point one-loop Passarino-Veltman integral functions of reference[18][19]. The integral functions are defined as follows:

The two-point integrals are:

$$\{B_0; B_\mu; B_{\mu\nu}\}(p, m_1, m_2) = \frac{(2\pi\mu)^{4-n}}{i\pi^2} \int d^n q \frac{\{1; q_\mu; q_\mu q_\nu\}}{[q^2 - m_1^2][(q+p)^2 - m_2^2]}, \qquad (A.a.1)$$

The function B_μ should be proportional to p_μ:

$$B_\mu(p, m_1, m_2) = p_\mu B_1(p, m_1, m_2) \qquad (A.a.2)$$

Similarly we get:

$$B_{\mu\nu} = p_\mu p_\nu B_{21} + g_{\mu\nu} B_{22} \qquad (A.a.3)$$

We denote $\bar{B}_0 = B_0 - \Delta$, $\bar{B}_1 = B_1 + \frac{1}{2}\Delta$ and $\bar{B}_{21} = B_{21} - \frac{1}{3}\Delta$. with $\Delta = \frac{2}{\epsilon} - \gamma + \log(4\pi)$, $\epsilon = 4 - n$. μ is the scale parameter. And the three-point and four-point integrals can be obtained similarly.

The numerical calculation of the vector and tensor loop integral functions can be traced back to the four scalar loop integrals A_0, B_0, C_0 and D_0 in Ref.[18][19] and the references therein.

B. Self-energy part of the amplitude.

The amplitude of self-energy diagrams δM_s (Fig.1.(a)) can be decomposed into t-channel M_s^t and u-channel terms M_s^u. We will just give the expressions of t-channel, and

u-channel can be obtained from t-channel, changing t into u and exchanging all indices and arguments of the incoming photons. The amplitude M_s^t can be expressed as:

$$\delta M_s^t = \delta M_s^{t(a)} + \delta M_s^{t(b)} + \delta M_s^{t(c)} \qquad (A.b.1)$$

where

$$\begin{aligned}\delta M_s^{t(a)} &= \frac{-4\pi i\alpha Q_c Q_t}{(t-m_t^2)(t-m_c^2)}\epsilon^\mu(p_3)\epsilon^\nu(p_4)\bar{u}(p_1)\gamma_\mu \\ &\quad (\not{p}_1 - \not{p}_3 + m_t)\left[\Sigma(p_1-p_3)\right](\not{p}_1 - \not{p}_3 + m_c)\gamma_\nu v(p_2), \qquad (A.b.2)\end{aligned}$$

$$\begin{aligned}\delta M_s^{t(b)} &= \frac{-4\pi i\alpha Q_c^2}{(m_t^2-m_c^2)(t-m_c^2)}\epsilon^\mu(p_3)\epsilon^\nu(p_4)\bar{u}(p_1)\Sigma(p1)(\not{p}_1 + m_c)\gamma_\mu \\ &\quad (\not{p}_1 - \not{p}_3 + m_c)\gamma_\nu v(p_2), \qquad (A.b.3)\end{aligned}$$

$$\begin{aligned}\delta M_s^{t(c)} &= \frac{-4\pi i\alpha Q_t^2}{(t-m_t^2)(m_c^2-m_t^2)}\epsilon^\mu(p_3)\epsilon^\nu(p_4)\bar{u}(p_1) \\ &\quad \gamma_\mu(\not{p}_1 - \not{p}_3 + m_t)\gamma_\nu(-\not{p}_2 + m_t)\Sigma(-p2)v(p_2). \qquad (A.b.4)\end{aligned}$$

where the quark electric charge $Q_c = Q_t = 2/3$, $\alpha = 1/137.04$ and $\Sigma(p)$ is defined as

$$-i\Sigma(p) = H_L \not{p} P_L + H_R \not{p} P_R - H_L^S P_L - H_R^S P_R \delta_{kl}, \qquad (A.b.5)$$

with

$$H_R = -i\Sigma_L, \qquad (A.b.6)$$

$$H_R = -i\Sigma_R, \qquad (A.b.7)$$

$$H_L^S = 0, \qquad (A.b.8)$$

$$H_R^S \;=\; 0, \qquad (A.b.9)$$

where

$$\Sigma_L \;=\; -\frac{i}{16\pi^2}\lambda^{'}_{i2j}\lambda^{'}_{i3j}(B_1[-p, m_{q_j}, m_{\tilde{l}_i}] + B_1[-p, m_{l_i}, m_{\tilde{q}_j}]), \qquad (A.b.10)$$

$$\Sigma_R \;=\; -\frac{iC_R}{16\pi^2}\lambda^{''}_{2jk}\lambda^{''}_{3jk}(B_1[-p, m_{q_j}, m_{\tilde{q}_k}] + B_1[-p, m_{q_k}, m_{\tilde{q}_j}]), \qquad (A.b.11)$$

where i and j, k are generations of leptons and quarks respectively, $C_R = 2$.

The amplitude from vertex diagrams and box terms can be obtained in a similar way from Fig.1.(b,c); however, it is very complex, so we do not express them here. For a hint of its structure, compare with Ref.[20]

References

[1] H.E. Haber and G.L. Kane, Phys. Rep. **117**(1985)75; J.F. Gunion and H.E. Haber, Nucl. Phys. **B272**(1986)1.

[2] G.Farrar and P.Fayet, Phys. Lett. **B76**(1978)575.

[3] L.J. Hall and M. Suzuki, Nucl. Phys. **B231**(1984)419.

[4] C.S. Aulakh, R.N. Mohapatra, Phys. Lett. **119B**(1982)136; J. Ellis, G. Gelmini, C. Jarlskog, G.G. Ross and J.W.F. Valle, Phys. Lett. **150B**(1985)142; G.G Ross and J.W.F. Valle, Phys. Lett. **151B**(1985)375; A. Santamaria and J.W.F. Valle, Phys. Lett. **195B**(1987)423.

[5] Y. Fukuda et al, Phys. Rev. Lett., **81**(1998)1562.

[6] C.Adloff et al, Z.Phys. **C74**(1997)191; J.Breitweg et al, Z.Phys. **C74**(1997)207; J.Butterworth and H.Dreiner, Nucl. Phys. **B397**(1993)3.

[7] S.Weinberg, Phys. Rev. **D26**(1982)287; P. Roy, TIFR/TH/97-60; D.K. Ghosh, S. Raychaudhburi and K. Sridbar, Phys. Lett. **B396**(1997)177; K. Agashe and M. Graesser, Phys. Rev. **D54**(1996)4445; K. Huitu, J. Maalampi, M.Raidl and A.Santamaria, Phys.Lett. **B430**(1998)355; J-H. Jiang, J.G. Kim and J.S. Lee, Phys. Rev. **D55**(1997)7296; Phys. Lett. **B408**(1997)367; Phys. Rev. **D58**(1998)035006, G. Bhattacharyya, D. Choudhury and K. Sridhar, Phys. Lett. **B355**(1995)193, J. Ferrandis, Phys. Rev. **D60**(1999)095012, M. A. Diaz, J. Ferrandis, J. C. Romao and J. W. F. Valle, Phys. Lett. **B453**, M. A. Diaz, J. Ferrandis, J. C. Romao and J. W. F. Valle, hep-ph/9906343, M. A. Diaz, J. Ferrandis and J. W. F. Valle, hep-ph/9909212, B. C. Allanach, A. Dedes and H. K. Dreiner, Phys. Rev. **D60**(1999)075014, S. Bar-Shalom, G. Eilam and J. Wudka, Phys.Rev. **D59**(1999)035010, S. Bar-Shalom, G. Eilam and A. Soni, hep-ph/9812518.

[8] R. Barbier et.al, hep-ph/9810232; B. Allanach et. al, hep-ph/9906224

[9] C.S. Huang et al, Phys. Lett. **B452**(1999)143.

[10] K.J. Abraham, K. Whisnant and B.-L. Young, Phys. Lett. **B419**(1998)381

[11] C.D. Froggatt and H.B. Nielsen, Nucl. Phys. **B147**(1979)277

[12] V.Telnov, Nucl. Instrum. Meth. **A294**(1990)72; L. Ginzburg, G. Kotkin and H. Spiesbergerm, Fortschr. Phys. **34** (1986)687.

[13] D.K. Ghosh, R.M. Godbole and S. Raychaudhuri, Z. Phys. **C75**(1997)357.

[14] S.Dimopoulos, G.F.Giudice and N.Tetradis, Nucl.Phys.**B454**(1995)59; F. Gabbiani et al, ROM2F/96/21.

[15] D. Atwood et al. Phys. Rev. **D53**(1996)1199; W-S. Hou and G-L. Lin, Phys. Lett. **B379**(1996)261; Y. Jiang, M-l. Zhou, W-G. Ma, L. Han, H. Zhou and M. Han, Phys. Rev. **D57**(1998)4343.

[16] R. Hempfling, Nucl. Phys. **B478**(1996)3; B. Mukhopadhay and S. Roy, Phys. Rev. **D55**(1997)7020.

[17] K.Cheung, Phys. Rev. **D47**(1993)3750; ibid. 50(1994)1173.

[18] Bernd A. Kniehl, Phys. Rep. **240**(1994)211.

[19] G. Passarino and M. Veltman, Nucl. Phys. **B160**(1979)151.

[20] Z-H.Yu, H.Pietschmann, W-G.Ma, L.Han and Y.Jiang, Euro. Phys. **C9**(1999)463.

Figure Captions

Fig.1 Feynman diagrams of $\gamma\gamma \to t\bar{c}$ subprocess. Fig.1 (a): Self-energy diagrams. Fig.1 (b): Vertex diagrams Fig.1 (c): Box diagrams (only t-channel). Dashed lines represent sleptons and squarks.

Fig.2 Cross section of $e^+e^- \to \gamma\gamma \to t\bar{c} + c\bar{t}$ as function of c.m.energy $\sqrt{s}$ with $\lambda''_{323}\lambda''_{223} =$ 0.625 solid line for $m_{\tilde{l}} = m_{\tilde{q}} = 100\ GeV$, and dashed line for $m_{\tilde{l}} = m_{\tilde{q}} = 150\ GeV$.

Fig.3 Cross section of $e^+e^- \to \gamma\gamma \to t\bar{c} + c\bar{t}$ as function of c.m.energy $\sqrt{s}$ with $\lambda'_{333}\lambda'_{323} =$ 0.096 solid line for $m_{\tilde{l}} = m_{\tilde{q}} = 100\ GeV$, and dashed line for $m_{\tilde{l}} = m_{\tilde{q}} = 150\ GeV$.

Fig.4 Cross section of $e^+e^- \to \gamma\gamma \to t\bar{c} + c\bar{t}$ at c.m.energy $\sqrt{s} = 500\ GeV$ as function of $\lambda''_{323}\lambda''_{223}$. solid line for $m_{\tilde{l}} = m_{\tilde{q}} = 100\ GeV$, and dashed line for $m_{\tilde{l}} = m_{\tilde{q}} = 150\ GeV$.

Fig.5 Cross section of $e^+e^- \to \gamma\gamma \to t\bar{c} + c\bar{t}$ at c.m.energy $\sqrt{s} = 500\ GeV$ as function of $\lambda'_{333}\lambda'_{323}$. solid line for $m_{\tilde{l}} = m_{\tilde{q}} = 100\ GeV$, and dashed line for $m_{\tilde{l}} = m_{\tilde{q}} = 150\ GeV$.

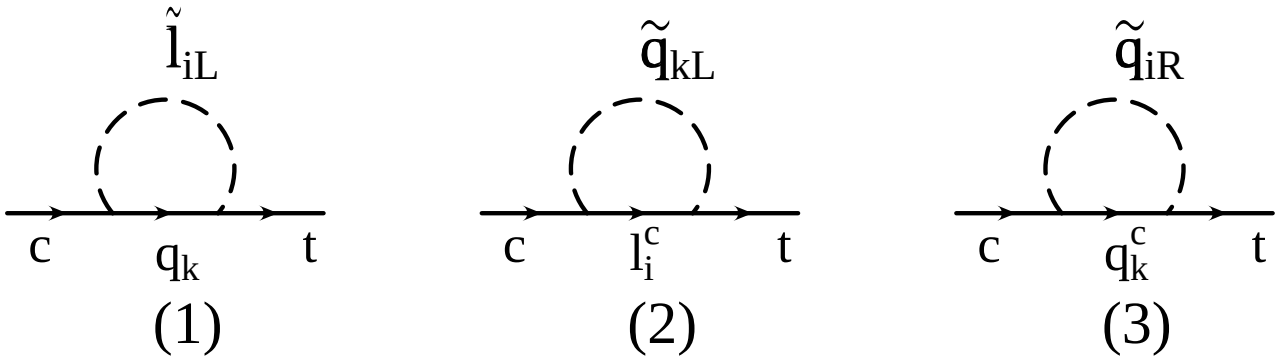
$\tilde{l}_{iL}$
c
q_k
t
(1)
$\tilde{q}_{kL}$
c
l_i^c
t
(2)
$\tilde{q}_{iR}$
c
q_k^c
t
(3)

Fig.1 (a)

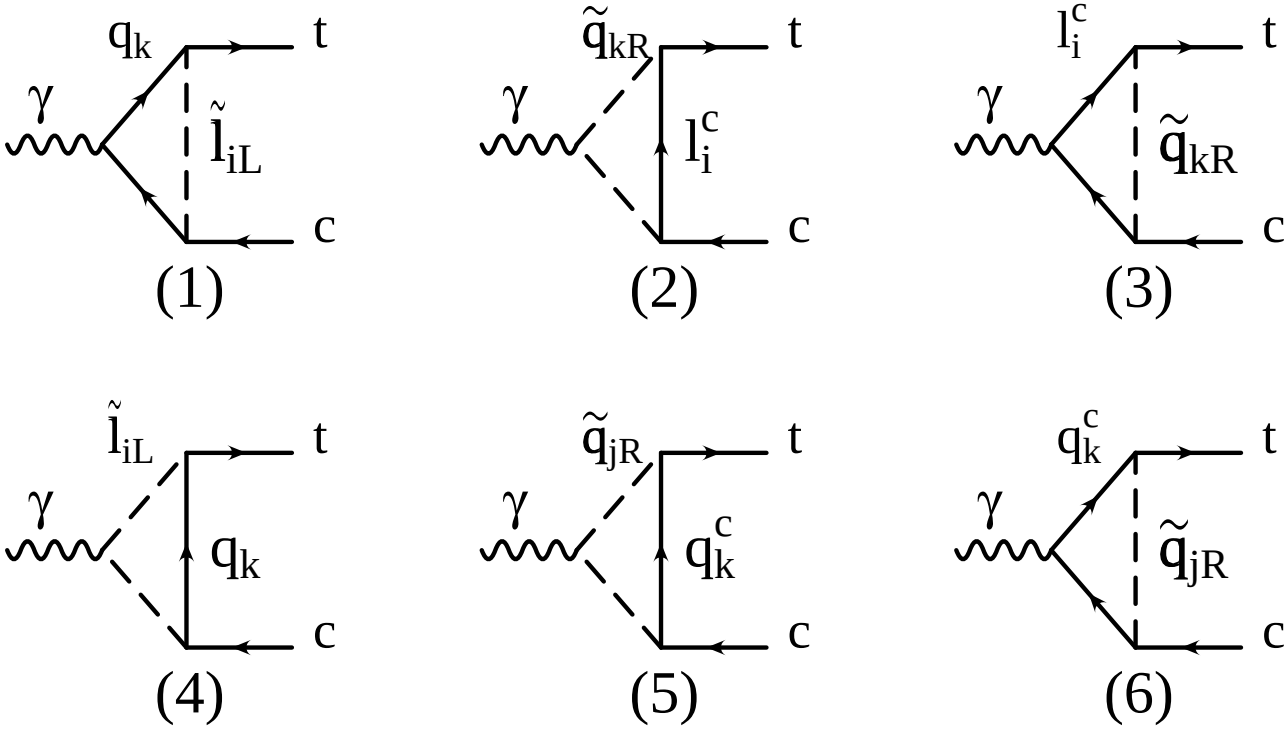
q_k
t
γ
$\tilde{l}_{iL}$
c
(1)
$\tilde{q}_{kR}$
t
γ
l_i^c
c
(2)
l_i^c
t
γ
$\tilde{q}_{kR}$
c
(3)
$\tilde{l}_{iL}$
t
γ
q_k
c
(4)
$\tilde{q}_{jR}$
t
γ
q_k^c
c
(5)
q_k^c
t
γ
$\tilde{q}_{jR}$
c
(6)

Fig.1 (b)

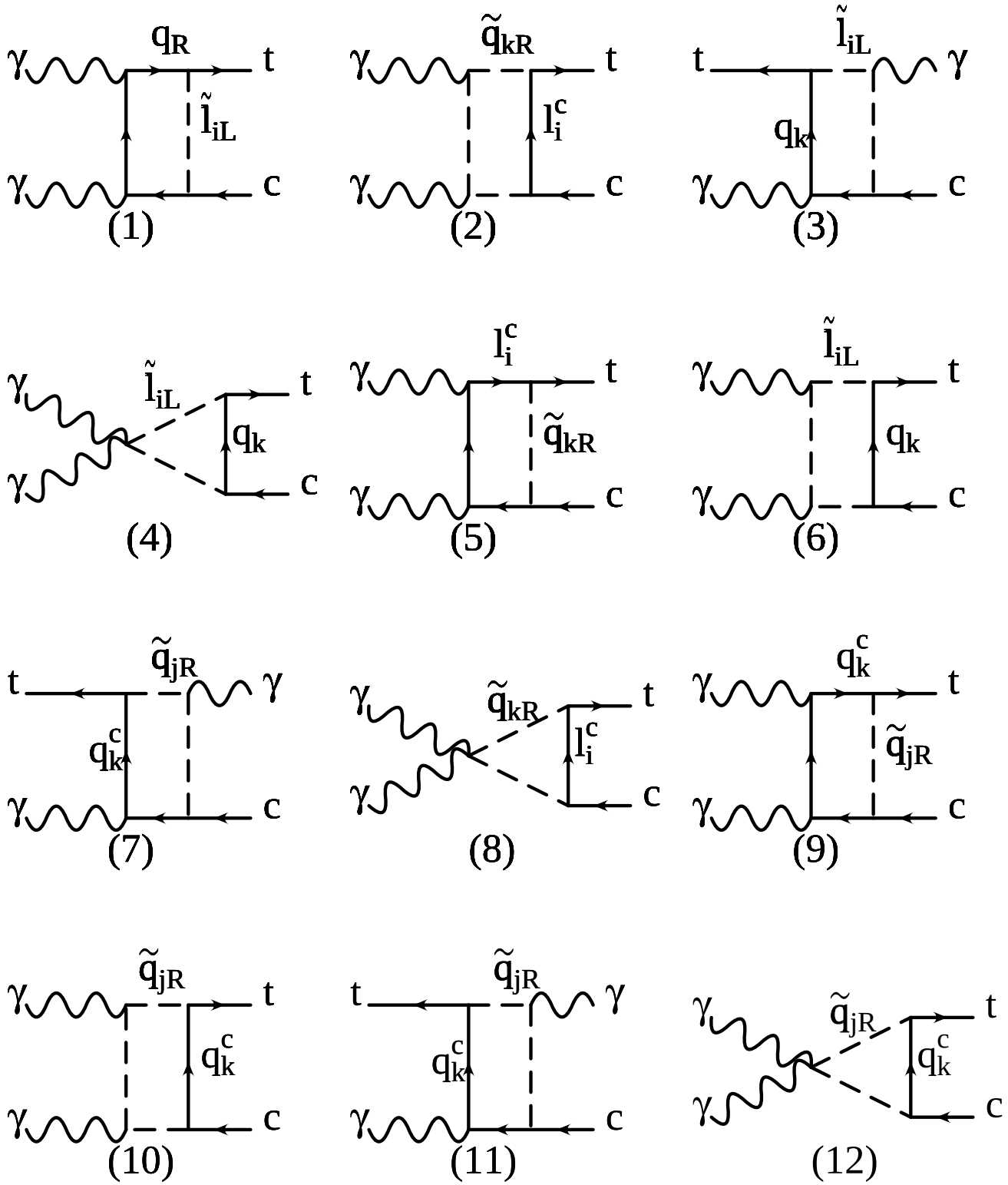
γ
γ
q_R
t
$\tilde{l}_{iL}$
c
(1)
$\tilde{q}_{kR}$
l_i^c
(2)
$\tilde{l}_{iL}$
q_k
(3)
(4)
l_i^c
$\tilde{q}_{kR}$
(5)
(6)
$\tilde{q}_{jR}$
q_k^c
(7)
(8)
(9)
(10)
(11)
(12)

Fig.1 (c)

Fig.2

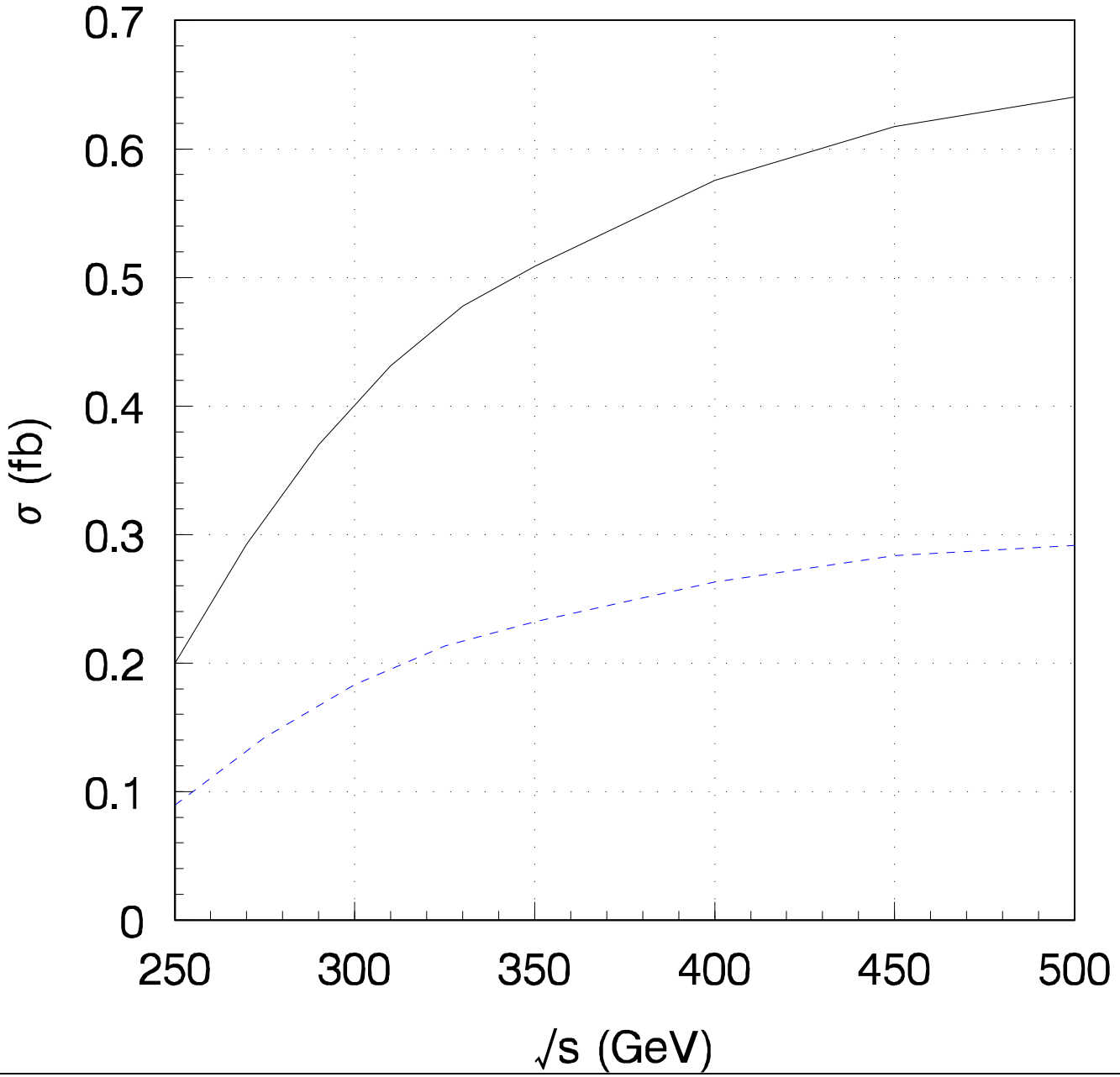

Fig.3

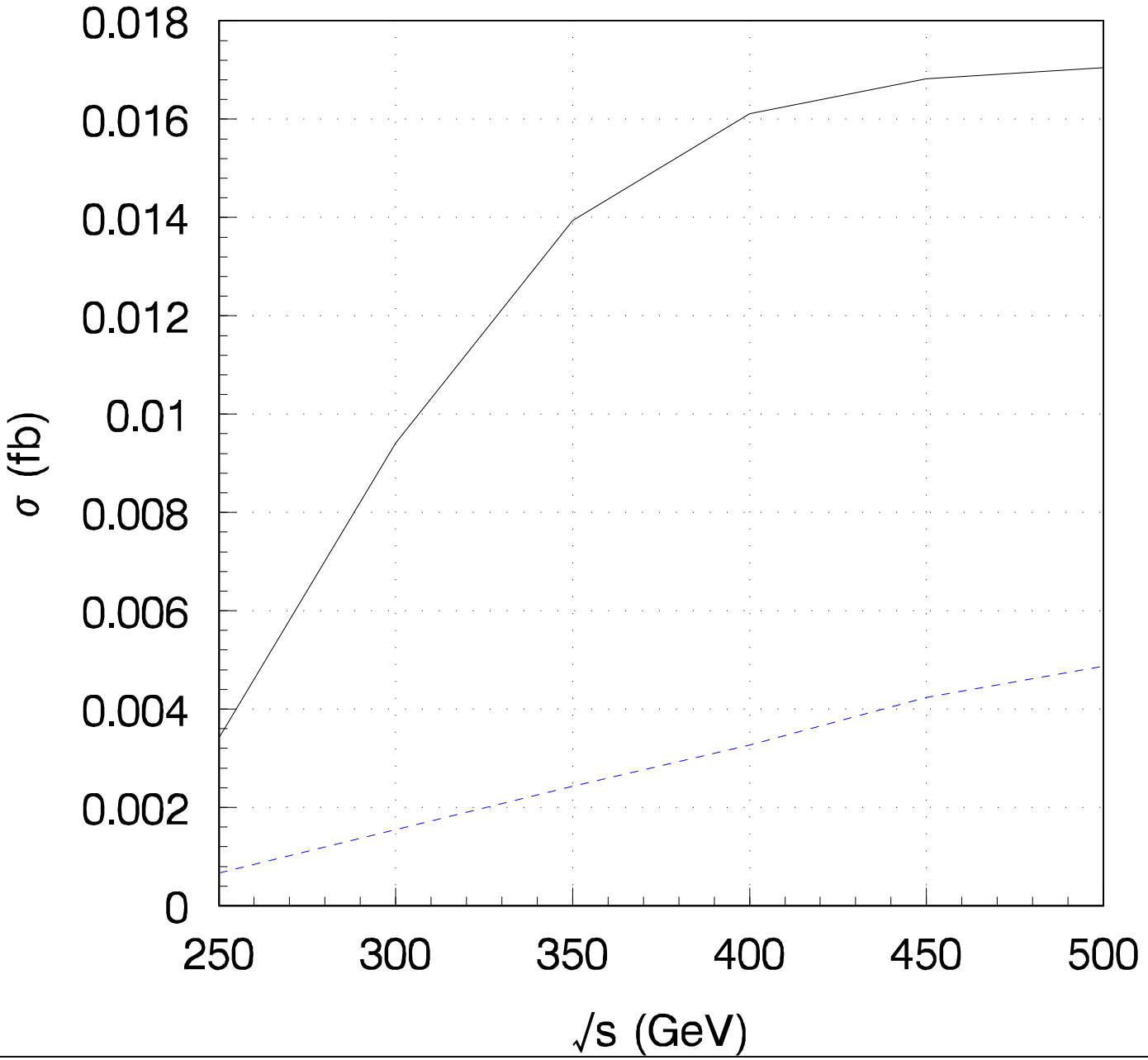
0.018
0.016
0.014
0.012
0.01
0.008
0.006
0.004
0.002
0
σ (fb)
250
300
350
400
450
500
√s (GeV)

Fig.4

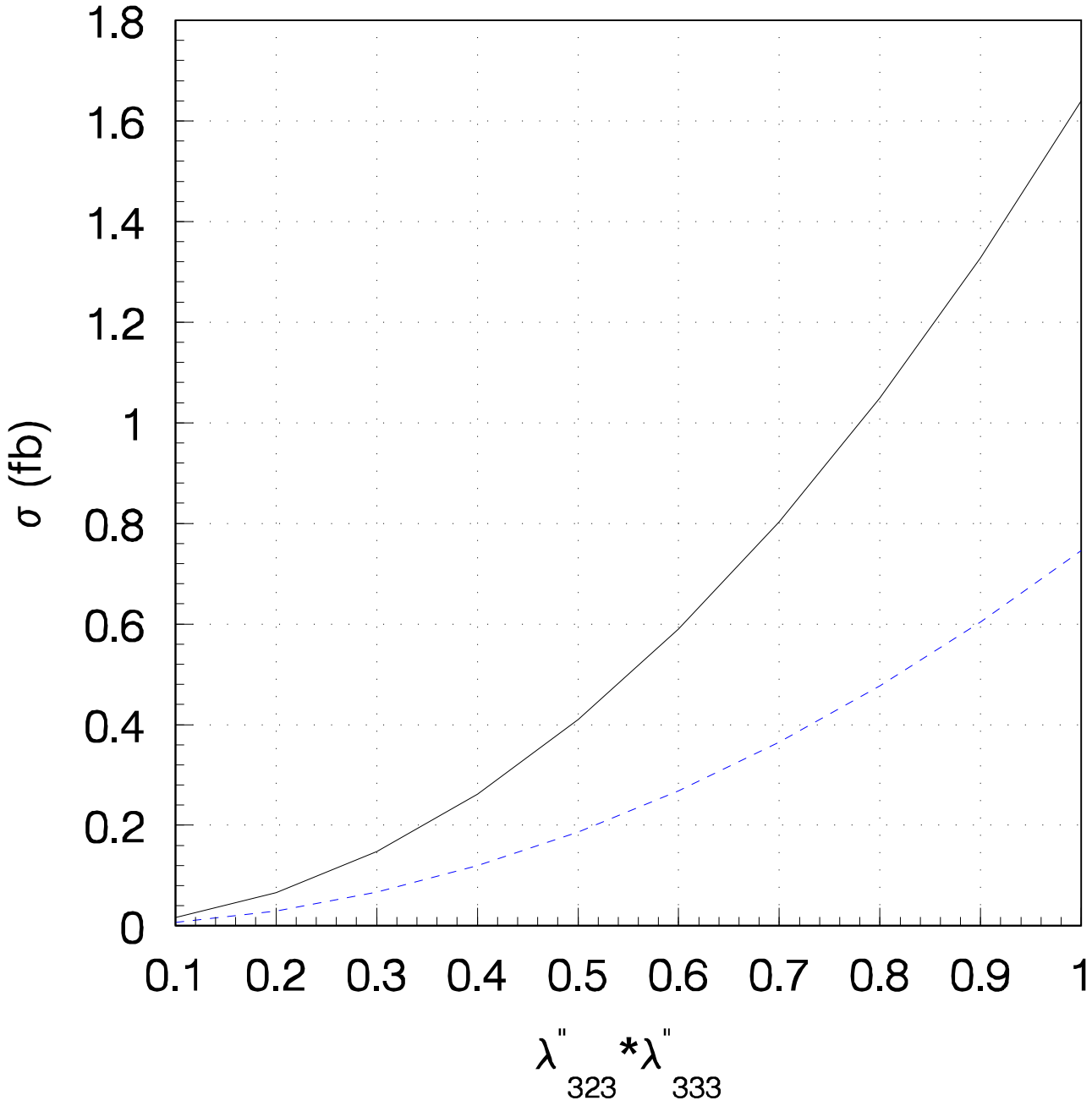

Fig.5